

CFD Simulation of Dry and Wet Pressure Drops and Flow Pattern in Catalytic Structured Packings

Maryam Mazarei Sotoodeh, Morteza Zivdar*
and Rahbar Rahimi

*Department of Chemical Engineering, University of Sistan and Baluchestan,
Zahedan 98164-161, Iran*

(Received 2016.07.11, Accepted 2017.05.24)

Abstract

Type of packings and characteristics of their geometry can affect the flow behavior in the reactive distillation columns. KATAPAK SP is one the newest modular catalytic structured packings (MCSP) that has been used in the reactive distillation columns, recently. However, there is not any study on the hydrodynamics of this packing by using computational fluid dynamics. In the present work, a 3D VOF model was developed to evaluate dry and wet pressure drops of catalytic structured packings, MCSP-11 and 12. The module of MCSP is made of alternating vertical layers of structured packing sheets (Mellapak Plus) and catalyst bags. The goal of this paper is to illustrate the effect of geometry on the hydrodynamics and characterization of flow in the MCSP modules. Results showed that the mean relative errors for prediction of dry and wet pressure drops were 17% and 7% for MCSP-11 and 11% and 12% for MCSP-12, respectively. According to CFD results, pressure drop in closed channels was higher than that in open channels. The catalyst bags were simulated as porous media. The simulation led to determination of the liquid velocity distribution in the catalyst bags.

Keywords

Reactive separation;
Modular catalytic structured
packing;
Mellapak Plus;
Multiphase model;
Hydrodynamic;
Computational fluid dynam-
ics.

1. Introduction

Reactive separations¹, in which chemical reaction and separation take place in one unit, are becoming more important in several areas of chemical engineering [1, 2]. These processes have many advantages over conventional methods (reactor-separator systems), especially by reducing investment and operational

costs. Therefore, in many cases, the use of these systems is preferred. Despite all the benefits of reactive separation, there are some limitations, which are summarized in Table 1 [1, 3, 4].

Due to high complexity and lack of commend in RS process, the need for further investigation in this area can be seen. Due to the cost of hydrodynamic experiments and various internal equipment (including various packing and catalysts), the use of CFD simulation has led to wider research on various types of packing and synthesis. Although numerous laboratory studies have been published in the field of reactive separation [5-

* Corresponding Author.

Tel./Fax: +989153414268

Email: mortaza@hamoon.usb.ac.ir (M. Zivdar)

¹ RS

14], few studies have been reported by using computational fluid dynamics. Van Baten et al. [15] studied the hydrodynamics of a reactive distillation sieve tray column in which the catalyst containing wire-gauze envelopes were disposed along the liquid flow direction. A 3D two-phase model was developed to determine liquid clear height on the tray as a function of tray geometry and operating conditions. A 3D steady-state one-phase model was presented by Kloker et al. [2] to obtain the influence of different catalytic internals on reactive distillation of n-hexyl acetate from hexanol and acetic acid. Egorov et al. [16] proposed a new modeling methodology for RS, which exploited a combination of modern CFD facilities and the rate-based process simulation approach. Hydrodynamics and mass transfer correlations were obtained by using CFD simulations. Zivdar et al. [17] investigated the dry pressure drop within the catalyst packed channels of KATAPAK-S by using CFD simulations. Also, the gas flow path line in the packing sheet and elbows were presented. A 3D two-phase CFD model was established to study the separation performance of structured catalytic packing by Dai et al. [18]. Two types of structured catalytic packings (i.e., BH-1 and BH-2) were used in simulations. Liu et al. [19] analyzed the multi-scale structure of a reactive distillation column by Aspen Plus with Fluent software. The reactive distillation column was divided into four scales: column scale, tray scale, fluid mechanical scale, and molecule scale. Tray efficiency was calculated by using CFD simulations. Ding et al. [20] presented a 3D model for simulating the winpak-based modular catalytic structured packing by using CFD. The model was validated by both dry and irrigated pressure drops.

In recent years, some forms of catalytic packing, such as KATAPAK SP, have been introduced by the Sulzer Company. Experimental works on the hydrodynamics and reaction of KATAPAK SP modules (Modular Catalytic Structured Packing¹) were reported [21-26]. There has not been any research on this type of packing by using CFD simulation yet. Rahimi et al. [27] investigated the effect of geometry on the efficiency of sieve trays by CFD. Also, Zarei et al. [28] and Hosseini et al. [29] worked on the hydrodynamics of MVG trays and gas solid fluidized bed, respectively.

In the first part of this paper, a 3D VOF model is developed to evaluate dry and wet pressure drops of MCSP-11 and 12. The aim of this part is to illustrate the effect of geometry on the hydrodynamics and characterization of flow in the MCSP modules. In the second part, catalyst bags of MCSP are simulated as porous media. The results show the liquid velocity distribution in the catalyst bags.

2. MCSP Description

KATAPAK SP (MCSP) packings are relatively new structured catalytic packings from Sulzer Chemtech Company, which are used in reactive separation columns. These types of packings are composed of two distinct parts: separation section and reactive section. The MCSP module is made of alternating vertical layers of structured packing sheets and catalyst bags. The ratio of separation to reactive layers can vary to declare flexibility between separation and reaction processes. Usually, Mellapak or Mellapak Plus is used in separation section as separation layer. The reactive section is made of wire gauze envelopes containing Amberlyst 15 catalyst particles. The contact of gas and liquid happens in structured packing sheet, and the separation process is done in this layer. Only the liquid phase flows through reactive section and the reaction is carried out in contact with the catalyst particles. Fig. 1 shows the picture of MCSP-11 and 12. The suffixes 11 and 12 denote an alternating arrangement of one corrugated sheet with one catalyst bag and two corrugated sheets with one catalyst bag, respectively.

3. Model Development Method

3.1. Simulation

This paper presents a 3D steady-state VOF model to illustrate one-phase and two-phase flows in MCSP-11 and 12. As mentioned in section 1, there were some experimental results on the hydrodynamics of these packings. To validate the proposed model, the results of simulation were compared with the experimental results of Behrens [23]. Process flow diagram of experimental setup is shown in Fig. 2.

¹ MCSP

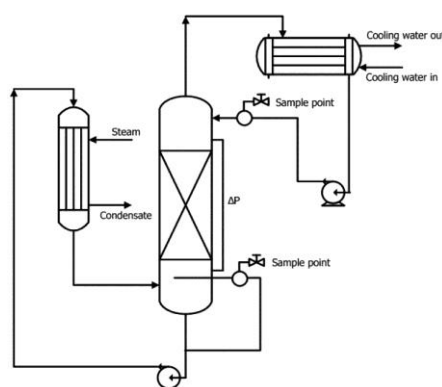
Table 1. advantages and limitations of reactive separations [1, 3, 4].

Advantages	limitations
Simplification or elimination of the separation system (capital savings)	Volatility constraints
Improved selectivity and reduced by-product formation	Residence time requirement
Significantly reduced catalyst requirement	Scale up to large flows
Avoidance of azeotropes	Process conditions mismatch
Heat integration benefits	The liquid phase reaction
Avoidance of hot spot formation	Long-lifetime catalysts strongly required

**Figure 1.** Schematic depiction of MCSP; left: MCSP-12, right: MCSP-11 [23]

The detailed characteristics of geometry, computational domains, and boundary conditions are presented in section 3.3. Because of the complicated geometry, lack of appropriate understanding of multi-scale phenomena in MCSP, and time-consuming simulations, several assumptions have been used in the simulations. The hydraulic parameters such as dry and wet pressure drops slightly change over simulation time. Also, they show a periodic or “quasi-steady state” manner. These parameters have some effect on the gas-liquid contact time and mass transfer rate between two phases. As these changes are negligi-

ble, the steady-state assumption is acceptable. Also, due to complicated geometry of catalyst particles in the reactive section, the Catalyst bags are assumed as porous media [16].

**Figure 2.** Process flow diagram [23]

The continuity and momentum equations are numerically solved for each phase. In single-phase flow, the air is used as gas phase and in two-phase analysis, air and water are assumed as the gas and liquid phases, respectively. Simulations are done at atmospheric pressure and ambient temperature. Therefore, one can neglect the use of energy balance equations. The fluids are assumed to be Newtonian, isothermal, and incompressible. Therefore, their physical properties are kept constant. Physical properties of water and air are listed in Table 2. Mass transfer and reactions as well as capillary rise are neglected in this part of research.

Table 2. Physical properties of air and water.

property	symbol	water	air
Density [kg/m ³]	ρ_L, ρ_G	998	1.2
Dynamic viscosity [Pa.s]	μ_L, μ_G	0.00115	1.82×10^{-5}
Surface tension [N/m]	σ_L	0.073	----
Static contact angel of air and steel [deg]		70	

The maximum dynamic liquid hold-up is reached when the void fraction of the catalyst containing pocket is just completely filled with flowing liquid. This point is characterized as the catalytic load point, which is a function of physical properties of the liquid, particle size, and void fraction of the bed [23]. Simulations are done at the liquid load point for both geometries. All the walls are assumed impermeable; therefore, the liquid cannot move from catalyst bags to corrugated sheets and vice versa.

3.2. Governing equations

The VOF model is well suited for tracking the interface between the two immiscible phases, which has been validated by many researchers for gas-liquid CFD simulations of structured packing [30, 31, 32]. Therefore, in the present study, it is used to predict two-phase flow in the structured packings and the effect of surface tension along the interface between the phases. The mass transfer between the immiscible water and air phases is neglected.

In this model, no relative velocity between phases is considered and all phases share a single set of momentum equations throughout the domain. But, the volume of phases in each computational cell is tracked as well. The resulting velocity in each cell is the mass averaged values of the velocity of phases that are presented in the cell. The corresponding momentum balance equation for the steady-state two-phase flow is given as follows:

$$\nabla \cdot (\rho \vec{v} \vec{v}) = -\nabla \cdot P + \nabla \cdot [\mu (\nabla \vec{v} + \vec{v}^T)] + \rho \vec{g} + \vec{F} \quad (1)$$

Eq. (1) involves the volume fractions of both phases that enter through physical properties of phases, such as density and viscosity. Hence, the phase averaged properties are given as:

$$\rho = \alpha_1 \rho_1 + \alpha_2 \rho_2 \quad (2)$$

$$\mu = \alpha_1 \mu_1 + \alpha_2 \mu_2 \quad (3)$$

where ρ and α are density and volume fraction, and subscripts correspond to the phases.

In each control volume, the summation of volume fractions of all phases is equal to unity. That is:

$$\sum_{i=1}^n \alpha_i = 1 \quad (4)$$

The tracking of the interface is done in cells where the volume fraction is different from 0 or 1. If a cell is completely filled with one phase, the volume fraction of that phase in the cell is equal to unity ($\alpha = 1$) and the cell is considered to be in the main flow region of that phase. A cell is considered to be on the interface (free surface) when the value of volume fraction is between 0 and 1 ($0 < \alpha < 1$).

The tracking of the interface(s) between the phases is accomplished by the solution to a continuity equation for the volume fraction of one (or more) of the phases. For the i^{th} phase, it can be written as:

$$\nabla \cdot (\alpha_i \rho_i \vec{v}) = 0 \quad (5)$$

The VOF model accounts for the effect of surface tension along the interface between the phases. The continuum surface force (CSF) model is applied as surface tension model [30, 31]. This model was proposed by Brackbill et al. [33]. In the CSF model, a surface force is formulated to numerically model the surface tension effects at fluid interfaces having finite thickness [33]. The BSL model is used to solve the turbulent viscosity in the simulations [30, 31].

As mentioned above, in the computational domain, the catalyst bags are assumed as porous media. A momentum source term is added in the standard fluid flow equations and the porous medium is considered to be homogeneous and isotropic. The source term S_i is:

$$S_i = -\frac{\mu}{a} v_i + C_2 \frac{1}{2} \rho |v| v_i \quad (6)$$

where a is permeability and C_2 is the inertial resistance coefficient defined as:

$$a = \frac{d_p^2 \varepsilon_{CB}^3}{150(1 - \varepsilon_{CB})^2} (m^2) \quad (7)$$

$$C_2 = \frac{3.5(1 - \varepsilon_{CB})}{d_p \varepsilon_{CB}^3} (m^{-1}) \quad (8)$$

where d_p ($= 1\text{mm}$) is the diameter of catalyst particles used in catalyst bags and ε_{CB} is the void fraction, which is dependent on the type of catalytic structure module. The first and second terms in the right side of Eq. (6) represent the viscosity loss and inertial loss, respectively. These terms can be neglected in laminar flow when the fluid flows through a porous medium.

3.3. Computational domains and boundary conditions

The catalytic structured packings of Behrens [23] are used in the simulations. Computational domains containing a piece of MSCP are divided into three sections: a separation section in the middle and one catalyst bag on each side as reactive section. The domains were shown in Fig. 3. In MCSP-11, one sheet of Mellapak Plus is drawn as separation layer. In this situation, all of the channels of corrugated sheet are in the vicinity of catalyst bags. These channels are called closed channels. In MCSP-12, two sheets of Mellapak Plus are drawn between catalyst bags as separation layer. In this case, two types of channels are created:

closed channels and open channels. Open channels are the crisscrossing channels in the middle of two sheets.

There are three effective ratios in the structure of MCSP, which are known as channel ratio, cross sectional ratio, and volume fraction of the catalyst. These parameters differentiate both MCSP-11 and MCSP-12 and affect the pressure drop of modules and, consequently, the mass transfer and reaction performance of packing. The characteristics of geometries and ratios are shown in Table 3.

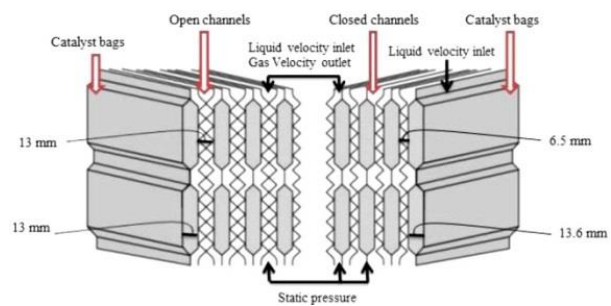


Figure 3. Simple schematic of computational domains; left: geometry of MCSP-11, right: geometry of MCSP12 [23].

Table 3. Geometrical characteristics of packings [23]

Property	Symbol	MCSP-11	MCSP-12
Cross sectional fraction	Γ	0.40	0.52
Volume fraction of catalyst	Λ	0.46	0.34
Channel ratio	X	0	0.5
Void fraction	ε_p	0.55	0.7
Thickness of catalyst-filled pockets	t_r	13.6 mm	13 mm
Height packing element	h_{pe}	200 mm	
Corrugation height	H	6.5 mm	
Corrugation base width	B	9.85 mm	
Corrugation angle	$\alpha_{e \text{ or } c}$	41°	
Overall corrugation angle	α	45°	
Catalyst diameter	d_p	1 mm	

The following terms are used in characterization of packings. The channel ratio is:

$$X = \frac{\text{number of open channels per packing layer}}{\text{total number of channels per packing layer}} \quad (9)$$

The vapor is not able to flow through the catalyst bags, because of their dense structure, so the cross sectional area available for the vapor is reduced. The cross sectional ratio is defined as:

$$\Gamma = \frac{\text{cross sectional area for separation section}}{\text{total cross sectional area}} \quad (10)$$

The volume fraction of catalyst ratio specifies the reaction performance compared to the separation performance. This ratio is determined as follows:

$$\Lambda = \frac{\text{volume occupied by the catalyst}}{\text{volume occupied by MCSP module}} \quad (11)$$

Computational domains are meshed by unstructured mesh. Mesh independency is done for computational domains. Several sizes of mesh, i.e., 0.2, 0.3, 0.35, 0.4, and 4.5 mm, are tested to make sure of numerical accuracy of simulations. Eventually, the size of 0.35mm is selected for separation section and the size of 0.3mm is selected for the reactive section based on the simulation results. The total numbers of meshes for MCSP-11 and MCSP-12 are 3508724 and 7644644, respectively.

Typically, the relative error between two successive iterations is specified by using convergence criteria of 10^{-6} and 10^{-4} for each scaled residual component in one-phase and two-phase simulations, respectively. The computational time required for each two-phase simulation is more than one week on a core i7 CPU running on an eight-core 2.67 GHz with 18.0 GB of RAM.

On the bottom of domains, static pressure is selected for catalyst bags and structured packing sheets. At the top, liquid inlet velocity and gas outlet velocity are specified for both domains. No slip wall boundary condition is selected for the liquid flow and free slip wall boundary condition is used for the gas phase. Hydrophobicity and smoothness of the walls and the properties of liquid (such as density, surface tension, and viscosity) can affect the contact angle between liquid and solid. Contact angle of 70° is assumed between water and walls [30, 31, 32, 33].

4. Results and Discussion

3D steady-state VOF simulations are done for investigating dry gas and two-phase flows in MCSP-11 and 12. The results of simulations are validated by Behrens [23] experimental data. In section 4.1, one-phase flow is discussed. Dry pressure drops for both geometries are presented and compared with experimental results. Also, the effect of geometry (Mellapak Plus) on the gas flow direction is shown. Two-phase flow pattern and wet pressure drop results are presented in section 4.2. Liquid velocity contour in the middle of catalyst bag is shown in section 4.3.

4.1. One-phase flow

The dry pressure drop is the first parameter in the validation of the hydrodynamic simulations of

structured packings. Simulations are done in different F_s for two geometries. The range of F_s is 0.58 up to 2.44 ($\text{m/s} (\text{kg/m}^3)^{0.5}$). Fig. 4 compares the simulated pressure drop with the experimental data. For MCSP-11 and 12, it can be seen that the simulated pressure drops are under- and over-predicted in all F_s , respectively. Although, the trends of simulated pressure drop vs. F_s exhibit the same behavior with experimental data for both geometries. On the other hand, by increasing the F_s , the pressure drop increases and vice versa.

Since the cross sectional fraction available for gas flow in the MCSP-12 is larger than that in the MCSP-11 (i.e. $\Gamma_{11} : \Gamma_{12} = 0.4 : 0.52$), the pressure drop of this packing is lower than that of the MCSP-11. The same trend was observed by Behrens [23].

Fig. 5 compares simulation and experimental dry pressure drops for all F_s in MCSP-11 and 12. The solid line in the figure denotes that the simulation pressure drop is equal to the experimental one and dotted lines over and under the solid line represent 15% deviations.

The simulation results are found in good agreement with experimental data and they show about 17% and 12% average deviations for MCSP-11 and 12, respectively.

It is clear in Fig. 6 that the gas flow transfers smoothly to the next vertical sheet due to vertical section between the sheets of Mellapak Plus. Therefore, the pressure drop in this packing is less than Mellapak. It confirms the findings of previous researchers such as Olujic et al. [32].

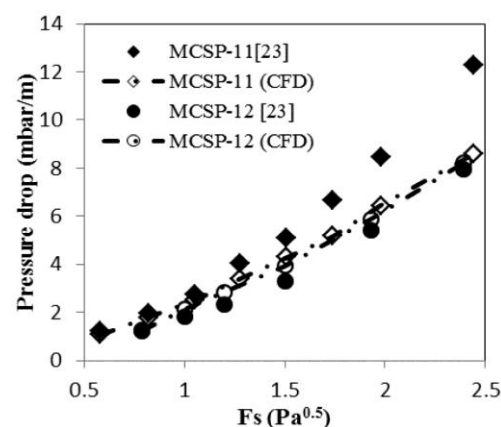


Figure 4. MCSP-11 dry pressure drop vs. F_s .

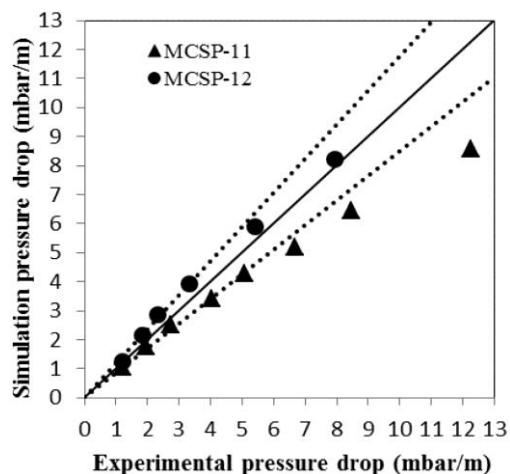


Figure 5. Simulation and Experimental pressure drops for all F_s in MCSP-11 and 12.

4.2. Two-phase flow

Liquid volume fraction on the channel walls in separation packing sheet is shown in Fig. 7a. It shows that the liquid distribution along the channels is not uniform. Moreover, more liquid is spread at the bottom of computational domain due to gas entrance. Similar liquid distributions are observed for different values of F-factor in both geometries.

Since the boundaries around the catalyst bag have been defined as impermeable walls, liquid velocity near the wall boundaries is zero, while it is uniform inside the bag. As can be seen in Fig. 7b, the last result is reached by assuming the catalyst bag as homogeneous and isotropic porous medium.

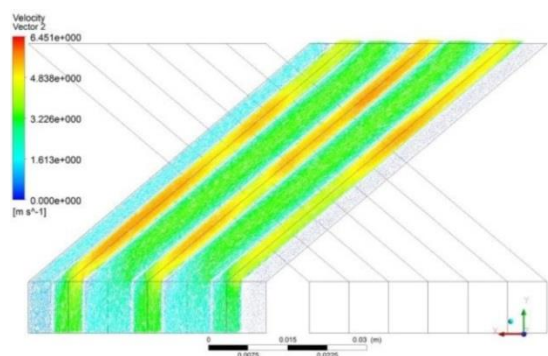


Figure 6. Gas velocity vector in the channels of MCSP-12.

The wet pressure drop within a certain range of F_s ($\approx 0.55 - 1.2 \text{ (m/s (kg/m}^3)^{0.5})$) is noticeable in Fig. 8. All the simulations are done at the liquid loading point. As expected, the pressure drop increases by increasing F_s .

Separation section in MCSP-11 includes only closed channels. Thus, the pressure and velocity profiles are the same in all channels. However, MCSP-12 contains both open and closed channels. Therefore, this difference leads to different pressure drop profiles in the channels of packing layer, which are shown in Fig. 9.

It is clear that pressure drop in the closed channels is approximately 70% higher than that in open channels. While, the pressure drop of separation section in MCSP-12 is between these two types of channel. As mentioned in section 3.3, the differences in the pressure drop profiles occur because of the difference in the nature of channels.

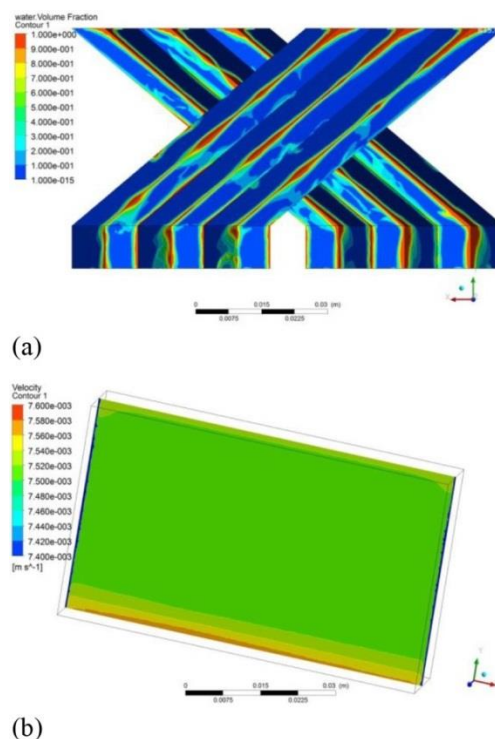


Figure 7. (a) Liquid volume fraction in the separation section, (b) Liquid velocity distribution in the center of catalyst bag.

The discrepancy between the simulation results and experimental data for MCSP-11 and 12 is

shown in a parity plot in Fig. 10. As explained in section 4.1, the solid line in the figure denotes that the simulation pressure drop is equal to the experimental one and dotted lines over and under the solid line represent 9% deviations. The mean relative errors of the simulations and experimental data for MCSP-11 and 12 are approximately 7% and 11%, respectively.

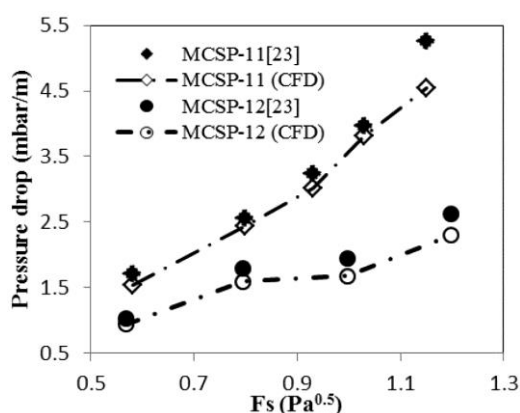


Figure 8. MCSP-11 and 12 wet pressure drops vs. F_s at liquid loading point.

5. Conclusions

KATAPAK SP (MCSP) packings are composed of two distinct parts: separation section and reactive section. The module of MCSP is made of alternating vertical layers of structured packing sheets and catalyst bags. The ratio of separation to reactive layers expresses flexibility between separation and reaction.

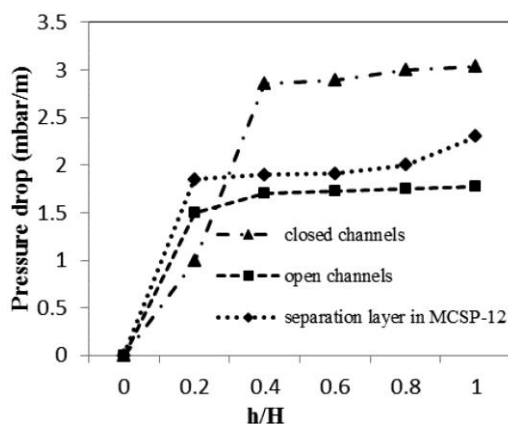


Figure 9. Pressure drop profile along the closed channels, open channels, and MCSP-12 separation sections.

In the present work, MCSP-11 and 12 are investigated to gain more information about the reactive separation internals. For this purpose, a 3D VOF model is used to study the hydrodynamics of catalytic structured packings by using CFD. Results exhibit the non-uniformity of the liquid distribution on the channel walls. In addition, the uniformity of liquid velocity in the catalyst bag is shown. This result is because of assuming the catalyst bag as homogeneous and isotropic porous medium.

Simulation results are used to calculate dry and wet pressure drops for both packings and validated by Behrens [23] experimental data. The simulation results for dry pressure drop reveal 17% and 12% deviations for MCSP-11 and MCSP-12, respectively. Also, the mean relative errors for prediction of wet pressure drop are 7% and 11% for MCSP-11 and MCSP-12, respectively.

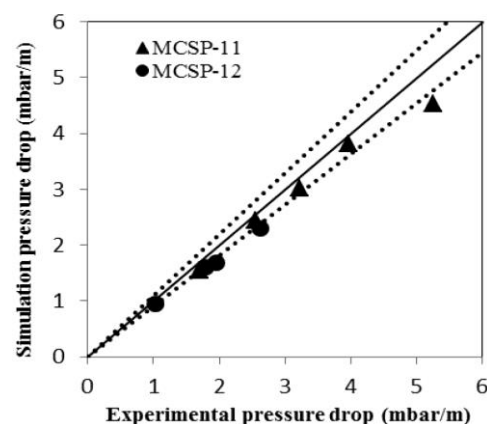


Figure 10. MCSP-12 wet pressure drop vs. F_s at liquid flow rate = $10 \text{ m}^3\text{hr}^{-1}$.

Moreover, the profiles of pressure drop in two types of MCSP-12 channels, i.e., closed channels and open channels, are presented. Results show that the pressure drop in closed channels is about 70% higher than that in the open channels. The differences in the pressure drop profiles occur because of the difference in the nature of channels.

Nomenclature

a	Permeability (m^2)
C_2	Resistance coefficient (m^{-1})
FS	Gas capacity factor ($\text{m/s}(\text{kg/m}^3)^{0.5}$)
t_R	Thickness of catalyst-filled pockets
d_p	Diameter of catalyst particle (mm)
P	Pressure (Pa)
g	Gravitational acceleration (m/s^2)
\vec{F}	Additional forces in the Navier–Stokes equations (N)
S	Source term (Pa m^{-1})
v	Velocity (m/s)

Greek letters

α	Overall corrugation angle
α_e	Corrugation angle
Γ	Cross sectional fraction
ε	Porosity, dimensionless
ε_p	Void fraction
Λ	Volume fraction catalyst
μ	Dynamic viscosity (Pa.s)
ρ	Density (kg/m^3)
σ	Surface tension (N/m)
X	Channel ratio

Subscripts

CB	Catalyst bag
G	Gas phase
L	Liquid phase

References

- Taylor, R. and Krishna, R. (2000). "Review-modeling reactive distillation." *Chemical Engineering Science*, Vol. 55, pp. 5183-5229.
- Klöker, M., Kenig, E.Y. and Górak, A. (2003). "On the development of new column internals for reactive separations via integration of CFD and process simulation." *Catalysis Today*, Vol. 79–80, pp. 479–48.
- Tuchlenski, A., Beckmann, A., Reusch, D., Dussel, R., Weidlich, U. and Janowsky, R. (2001). "Reactive distillation - industrial applications, process design & scale-up." *Chemical Engineering Science*, Vol. 56, pp. 387-394.
- Noeres, C., Kenig, E.Y. and Gorak, A. (2003). "Modelling of reactive separation process: reactive absorption and reactive distillation." *Chemical Engineering and Processing*, Vol. 42, pp. 157-178.
- Gonzalez, J.C. and Fair, J.R. (1997). "Preparation of Tertiary Amyl Alcohol in a Reactive Distillation Column. 1. Reaction Kinetics, Chemical Equilibrium and Mass-Transfer Issues." *Industrial and Engineering Chemistry Research*, Vol. 36, pp. 3833-3844.
- Gonzalez, J.C., Subawalla, H. and Fair, J.R. (1997). "Preparation of tert-Amyl Alcohol in a Reactive Distillation Column. 2. Experimental Demonstration and Simulation of Column Characteristics." *Industrial and Engineering Chemistry Research*, Vol. 36, pp. 3845-3853.
- Van Baten, J.M., Ellenberger, J. and Krishna, R. (2001). "Radial and axial dispersion of the liquid phase within a KATAPAK-S structure: experiments vs. CFD simulation." *Chemical Engineering Science*, Vol. 56, pp. 813-821.
- Schmitt, M., Hasse, H., Althaus, K., Schoenmakers, H., Götze, L. and Moritz, P. (2004). "Synthesis of n-hexyl acetate by reactive distillation." *Chemical Engineering and Processing*, Vol. 43, pp. 397–409.
- Schmitt, M., Scala, C., Moritz, P. and Hasse, H. (2005). "n-Hexyl acetate pilot plant reactive distillation with modified internals." *Chemical Engineering and Processing*, Vol. 44, pp. 677–685.
- Schmitt, M., Harbou, E., Parada, S., Grossmann, Ch. and Hasse, H. (2009). "New Equipment for Laboratory Studies of Heterogeneously Catalyzed Reactive Distillation." *Chemical Engineering Technology*, Vol. 32, No. 9, pp. 1313–1317.
- Bhatia, S., Ahmad, A.L., Mohamed, A.R. and Chin, S.Y. (2006). "Production of isopropyl palmitate in a catalytic distillation column: Experimental studies." *Chemical Engineering Science*, Vol. 61, pp. 7436–7447.
- Brehelin, M., Forner, F., Rouzineau, D., Repke, J.U., Meyer, X., Meyer, M. and Wozny, G. (2007). "Production of n-propyl acetate by reactive distillation Experimental and Theoretical Study." *Chemical Engineering Research and Design*, Vol. 85 (A1), pp. 109–117.
- Harbou, E., Schmitt, M., Parada, S., Grossmann, C. and Hasse, H. (2011). "Study of heterogeneously catalyzed reactive distillation." *Chemical Engineering and Processing*, Vol. 50, pp. 100–109.

- ously catalysed reactive distillation using the D+R tray- a novel type of laboratory equipment." *Chemical Engineering Research and Design*, Vol. 89, pp. 1271-1280.
14. Holtbruegge, J., Heile, S., Lutze, P. and Górak, A. (2013). "Synthesis of dimethyl carbonate and propylene glycol in a pilot-scale reactive distillation column: Experimental investigation, modeling and process analysis." *Chemical Engineering Journal*, Vol. 234, pp. 448-463.
 15. Van Baten, J.M., Ellenberger, J. and Krishna, R. (2001). "Hydrodynamics of reactive distillation tray column with catalyst containing envelopes: experiments vs. CFD simulations." *Cataysis. Today*, Vol. 66, pp. 233-240.
 16. Egorov, Y., Menter, F., Kloker, M. and Kenig, E.Y. (2005). "On the combination of CFD and rate-based modeling in the simulation of reactive separation processes." *Chemical Engineering and Processing*, Vol. 44, pp. 631-644.
 17. Zivdar, M., Rahimi, R., Nasr, M. and Haghshenasfard, M. (2005). "CFD Simulations of pressure drop in KATAPAK-S Structured Packing." *Iranian Journal of Chemical Engineering*, Vol. 2, No. 2.
 18. Dai, C., Lei, Zh., Li, Q. and Chen, B. (2012). "Pressure drop and mass transfer study in structured catalytic packings." *Separation and Purification Technology*, Vol. 98, pp. 78-87.
 19. Liu, J., Yang, B., Lu, S. and Yi, C. (2013). "Multi-scale study of reactive distillation." *Chemical Engineering Journal*, Vol. 225, pp. 280-291.
 20. Ding, H., Li, J., Xiang W. and Liu, C. (2015). "CFD simulation and optimization of Winpak-based modular catalytic structured packing." *Industrial and Engineering Chemistry Research*, Vol. 54, pp. 2391-2403.
 21. Gotze, L., Bailer, O., Moritz, P. and von Scala, C. (2001). "Reactive distillation with KATAPAK." *Cataysis. Today*, Vol. 69, pp. 201-208.
 22. Ratheesh, S. and Kannan, A. (2004). "Hold up and pressure drop studies in structured packings with catalysts." *Chemical Engineering Journal*, Vol. 104, pp. 45-54.
 23. Behrens M. (2006). "Hydrodynamics and Mass Transfer of Modular Catalytic Structured Packing." *Technische universiteit Delft*, Ph.D. thesis.
 24. Brunazzi, E. and Viva, A. (2006). "Experimental investigation of reactive distillation packing KATAPAK-SP 11: hydrodynamic aspects and size effect." *ICHEME Symposium*, No. 152, Italy.
 25. Viva, A., Aferka, A., Teye, D., Marchot, P., Crine, M. and Brunazzi, E. (2011). "Determination of liquid hold-up and flow distribution inside modular catalytic structured packings." *Chemical Engineering Research and Design*, Vol. 89, pp. 1414-1426.
 26. Fernandez, M. F., Barroso, B., Meyer, X., Meyer, M., Le Lann, M., Le Roux, G.C. and Brehelin, M. (2013). "Experiments and dynamic modeling of a reactive distillation column for the production of ethyl acetate by considering the heterogeneous catalyst pilot complexities." *Chemical Engineering Research and Design*, Vol. 91, pp. 2309-2322.
 27. Rahimi, R., Mazarei Sotoodeh, M. and Bahramifar, E. (2012). "The effect of tray geometry on the sieve tray efficiency." *Chemical Engineering Science*, Vol. 76, pp. 90-98.
 28. Zarei, T., Rahimi, R. and Zivdar, M. (2009). "Computational fluid dynamic simulation of MVG tray hydraulics" *Korean Journal of Chemical Engineering*, Vol. 26(5), pp.1213-1219.
 29. Hosseini, S.H., Rahimi, R., Zivdar, M. and Samimi, A. (2009). "CFD simulation of gas-solid bubbling fluidized bed containing FCC particles." *Korean Journal of Chemical Engineering*, Vol. 26(5), pp. 1405-1413.
 30. Hosseini, S.H., Shojae S., Ahmadi, G. and Zivdar, M. (2012). "Computational fluid dynamics studies of dry and wet pressure drops in structured packings." *Journal of Industrial and Engineering Chemistry*, Vol. 18, pp. 1465-1473.
 31. Shojae S., Hosseini, S. H., Rafati, A. and Ahmadi, G. (2011). "Prediction of the effective area in structured packings by computational fluid dynamics." *Industrial and Engineering Chemistry Research*, Vol. 50, pp. 10833-10842.
 32. Zhang, X., Yao, L., Qiu, L. and Zhang, X. (2013). "Three-dimensional computational fluid dynamics modeling of two-phase flow in a

structured packing column." *Chinese Journal of Chemical Engineering*, Vol. 21(9),pp. 959-966.

33. Brackbill, J. U., Kothe, D. B. and Zemach, C. (1992). "A Continuum Method for Modeling Surface Tension." *Journal of Computational Physics*, Vol. 100, pp. 335-354.
34. Olujic, Z., Behrens, M. and Spiegel, L. (2007). "Experimental characterization and modeling of the performance of a large-specific-area high-capacity structured packing." *Industrial and Engineering Chemistry Research*, Vol. 46, pp. 883-893.